PCCP

Accepted Manuscript

ROYAL SOCIETY OF CHEMISTRY

www.rsc.org/pccp

Removal of multi-substituted nitroaromatic pollutants by zero valent iron: a comparison of performance, kinetics, toxicity and mechanisms

Changjin Ou, Shuai Zhang, Jianguo Liu, Jinyou Shen*, Yan Liu, Xiuyun Sun,
Jiansheng Li, Lianjun Wang*

Jiangsu Key Laboratory for Chemical Pollution Control and Resources Reuse, School of Environmental and Biological Engineering, Nanjing University of Science and Technology, Nanjing 210094, Jiangsu Province, China

* **Corresponding author**:
Jinyou Shen, Tel./fax: +86 25 84303965, E-mail: shenjinyou@mail.njust.edu.cn or
Lianjun Wang, Tel./fax: +86 25 84315941, E-mail: wanglj@mail.njust.edu.cn

Abstract

Reductive degradation of three typical multi-substituted nitroaromatic pollutants by zero valent iron was comprehensively compared in terms of performance, kinetics, toxicity and mechanisms in this study. The results showed that 0.5 mM 2,4-dinitrochlorobenzene (DNCB), 2,4-dinitroanisole (DNAN) and 2,4-dinitrophenol (DNP) could be completely removed in the ZVI reduction system within 75 min, 90 min and 210 min, respectively. The pseudo first-order kinetics could well describe the reduction process of the three NACs by ZVI. The reduction rates of the three NACs followed in the order of DNCB>DNAN>DNP, which was further confirmed by density function theory computations analysis. Moreover, the acute toxicity of the three NACs effluent significantly decreased after treatment by ZVI. In addition, the mechanism investigation revealed that the selective reduction of nitro groups on the three NACs was closely related to the characteristic of the functional groups on the benzene rings. The results of this study would increase the comprehensive understanding in terms of the performance, kinetics, toxicity and mechanisms involved in the reduction of multi-substituted NACs by ZVI, thus benefit the effective treatment of wastewaters containing multi-substituted nitroaromatic pollutants by ZVI.

Keywords: Multi-substituted nitroaromatic compound; Zero valent iron; Density function theory computations; Selective reduction

1. Introduction

Nitroaromatic compounds (NACs) are used widely since they are the most important intermediate products for the manufacture of insecticides, pharmaceuticals, explosives, and dyes, et a.[1] NACs are of interest to environmental scientists because they are known or suspected to be human toxins, carcinogens and mutagens.[2] Moreover, some NACs are considered as hazardous substances and priority toxic pollutants by the United States Environmental Protection Agency (USEPA). Therefore, their presence in wastewater is severely regulated and effective treatment is highly requested.

Due to the pronounced electron-withdrawing character of the nitro groups on the benzene ring, NACs often harbor a highly electron deficient π-electron system.[3] Thus the electrophilic attack, which is usually the first step in direct oxidation, becomes more difficult for NACs. However, the NACs are subject to initial reductive transformation.[4,5] Under the anaerobic conditions, NACs can be readily transformed into their corresponding aromatic amines without cleaving the aromatic ring. Nevertheless, due to the low biodegradability and high toxicity of NACs on the active biomass, the biological anaerobic reduction of NACs is usually very slow and requires an electron donor to create the necessary reductive condition.[6] Therefore, for the reductive degradation of NACs, it is essential to develop the abiotic methods, which are both efficient and cost-effective.

Zero valent iron (ZVI), as an inexpensive, reliable and moderately strong reducing agent, has attracted great interest in wastewater treatment, soil remediation and groundwater purification.[7] In light of the findings from the previous studies, ZVI was well suited to reduce various oxidative organic compounds, such as halogenated organic compounds (HOCs), azo dyes and NACs, et al.[8-10] To enhance the reactivity of ZVI, bimetallic particles prepared by the deposition of a second transition metal on the iron surface, have been proven to be effective in the removal of these oxidative contaminants.[11] Comparing with ZVI, the bimetallic particles had several advantages, such as high reaction rate and alleviative deposition of corrosion products on the particle surface. In addition to the bimetallic particles, high carbon iron filings (HCIF), which was cost effective, has been employed for the dehalogenation reaction of various HOCs, such as 2-chloronaphthalene and 2,4,6-trichlorophenol.[12-14] In addition to the dehalogenation reaction, the hydrophobic HOCs were prone to be adsorbed on HCIF surface, which would further facilitate the dehalogenation of HOCs. HCIF materials with larger specific surface area had a promising potential for the removal of HOCs from wastewater. Moreover, the adoption of nanoscale zero valent iron (nZVI) for the removal of oxidative contaminants has also received increasing attention due to its higher surface area and higher reactivity than ZVI.[15] Recently, several studies have typically indicated that the combination of ZVI with other techniques, such as Fenton oxidation and bioprocess, has made great progress in the remediation of sites contaminated by various oxidative contaminants.[16-18] Hindrance to subsequent Fenton oxidation or biological oxidation could be overcame by reductive transformation of the nitro functional groups in the presence of ZVI.

Most of the previous studies on the reduction of NACs by ZVI focused on the preparation and performance of the ZVI material.[11,15] In addition, the mono-nitro aromatic compounds, such as nitrobenzene and *p*-nitrophenol, were often chosen as the model because of their simple structure, large quantities and potential environmental contamination.[19,20] However, the reduction of multi-substituted NACs in the presence of ZVI could be significantly affected by the functional groups on the benzene rings, since the difference of the functional groups might result in the difference in the physicochemical characteristics of NACs, such as the octanol/water partition coefficient (K_{ow}), the presence of hydrogen bond and the charge density of a given aromatic system, etc.[21] Although there was a need to clarify the impact of these characteristic parameters on the reduction of multi-substituted NACs by ZVI, so far a systematic and comprehensive investigation was still absent.

Thus, in this study, the reductive degradation of multi-substituted NACs by ZVI in terms of performance, kinetics, toxicity and mechanisms, was comprehensively compared in order to evaluate the role of the functional groups. 2,4-Dinitroanisole (DNAN), 2,4-dinitrochlorobenzene (DNCB) and 2,4-dinitrophenol (DNP), which coexisted in the DNAN-producing wastewater, were selected as the model multi-substituted NACs in this study.[4] The effect of the substituent type (namely chlorine (-Cl), methoxyl (-OCH_3) and hydroxyl (-OH), respectively) on the reduction performance of NACs was emphasized.

2. Materials and methods

2.1. Materials

DNAN, DNCB and DNP were obtained from Hubei Dongfang Chemical Co. Ltd (Hubei, China). 2-Amino-4-nitrophenol (2-A-4-NP), 2-nitro-4-aminophenol (2-N-4-AP), 2,4-diaminoanisole (DAAN), 2-nitro-4-aminochlorobenzene (2-N-4-ACB), 2-amino-4-nitrochlorobenzene (2-A-4-NCB) and 2,4-diaminochlorobenze (DACB) were purchased from Sun Chemical Technology Co. Ltd (Shanghai, China). 2-Nitro-4-aminoanisole (2-N-4-AAN), 2-amino-4-nitroanisole (2-A-4-NAN) and 2,4-diaminophenhenol (DAP) were purchased from Bepharm Co. Ltd (Shanghai, China). All of the above chemicals were of the analytical reagent grade.

ZVI powder with analytical purity was purchased from Sinopharm Chemical Reagent Co. Ltd (Shanghai, China), and used without further pretreatment. The surface area of the ZVI powder was determined to be 0.071 m^2/g by gas adsorption using Brunauer-Emmett-Teller (BET) analysis.

2.2. Reductive experiments

The reduction experiments were carried out in batch mode. A series of 150 mL serum bottles with butyl rubber stoppers was employed as batch reactors. 100 mL aqueous stock solution containing 0.5 mM DNCB, DNAN or DNP was placed in the serum bottles for batch experiment. The initial pH was adjusted to 3.0±0.1 using 0.1 M HCl solution, since NACs could be well reduced by the iron powder in the acid condition. To increase the electrical conductivity, 0.06% NaCl was added into these solution as electrolyte. The solutions were purged with nitrogen gas for at least 10 min to remove any residual dissolved oxygen. To maintain anaerobic conditions, the serum bottles were sealed immediately with butyl rubber stoppers after adding 0.2 g ZVI powder into these solutions. Then the serum bottles were placed on rotary shaker at 200 rpm and 30 ^oC for intensive mixing. During the reduction process, 15 ml of solution sample was withdrawn from serum bottles at desired time intervals and then were filtered through a 0.22 μm membrane (ANPEL Laboratory Technologies Inc., Shanghai, China) for immediate analysis. To maintain anaerobic condition well, the NACs solution in each serum bottle was used only once.

All of experimental runs were performed in triplicate and the results were reported as an average of the three independent determinations.

2.3. Analyses

DNAN, DNCB, DNP and their corresponding intermediate products were identified and quantified by high performance liquid chromatography (HPLC) (Waters 2996, Waters Incorporation, USA). The HPLC analysis was conducted according to our previous study.[4] The reductive intermediates of NACs were also identified by high-performance liquid chromatograph (HPLC)-mass spectrometer (MS) (Agilent 6410, Agilent Technologies Incorporation, USA), using Agilent Eclipse Plus-C18 columns (3.5μm, 2.1×150 mm). The mobile phase was a mixture of 55% methanol and 45% water pumped at a flow rate of 0.2 mL/min. The ESI and the ion-trap analyzer MS parameters were optimized to reach the best sensitivity for intermediates. The ^{1}HNMR was recorded on Bruker DRX 500, with dChloroform-d ($DCCl_3$) used as a reference. The total organic carbon (TOC) content was measured with a TOC analyzer (Elementar vario, Germany). Acute toxicity of the influent and effluent was evaluated according to OECD Guideline 203.[22] The results of the toxicity were expressed as $EC_{50,\ 48h}$ (%, V/V), the concentration responsible for the death in 50% of the tested Zebrafish population after exposure.

The charge densities of N atoms and N-O mayer bond order on the three NACs were calculated using density functional theory in Materials Studio Modeling 6.0^{TM} package, after minimizing the energy.[5]

2.4 Kinetic model development

Langmuir–Hinshelwood model (L–H model) was widely used to describe the solid–liquid heterogenerous reaction kinetics.[23] The equation was formulated as follows (Eq. (1)):

$$-\frac{dC}{dt} = r = \frac{kKC}{1+KC} \qquad (1)$$

where r was the degradation rate of the organic substrate (mM/min), k was the degradation kinetic constant (min^{-1}or mM/min), K was the adsorption equilibrium constant (L/mmol), C was the concentration of the substrate in the aqueous solution (mM) and t was the reaction time (min). The L–H model could be simplified into the pseudo first-order kinetic model (Eq. (2)) when limited reactive surface sites were occupied or the concentrations of the reactants were relatively low. The pseudo first-order rate constant (K_1, min^{-1}) equaled to kK. However, when the reactive surface sites were saturated or played a minor role in the reaction, the reaction might follow the pseudo zero-order kinetic model (Eq. (3)), and the pseudo zero-order rate constant (K_0, mM/min) equaled to k.

$$\ln(C_0/C_t)=K_1t \qquad (2)$$

$$C_0 - C_t = K_0t \qquad (3)$$

where C_0 (mM) is the initial concentration of NACs, C_t is the NACs concentration (mM) at reaction time t (min).

For the ZVI reduction reaction, if the adsorption of contaminants onto ZVI surface played a minor role in the reductive process, the contaminant removal often followed the pseudo zero-order kinetic model, otherwise pseudo first-order kinetic model was more appropriate for the removal kinetics.[24] However, it was very difficult to determine the adsorption of NACs onto the surface of ZVI because the adsorption and reductive reaction occurred simultaneously. Therefore, the removal kinetics of NACs in this study was assessed by both pseudo first-order kinetic model and pseudo zero-order kinetic model.

3. Results and discussion

3.1. Performance of NACs reduction by ZVI

As indicated in Fig. 1 and S1, complete degradation of DNCB, DNAN and DNP could be achieved in the ZVI reduction system within 75 min, 90 min and 210 min, respectively. During the DNCB reduction process, the maximum accumulated concentrations of 2-N-4-ACB and 2-A-4-NCB were 0.273±0.002 mM and 0.018±0.001 mM, respectively, indicating that 2-N-4-ACB was the main intermediate (Fig. 1a and S1a). The concentration of the final reduction product, namely DACB, increased over time, from the initial 0 to final 0.369±0.015 mM. However, no *m*-phenylenediamine was detected in the effluent of DNCB reduction system, indicating that further dehalogenation of DACB was quite difficult in ZVI reduction system based on Fe^0. However, dehalogenation easily occurred in the catalytic reduction system based on high carbon iron filings (HCIF) or bimetallic nanoparticles.[13,25,26] The result was also consistent with our previous study, where DACB was also found to be the final product in the ZVI reduction system.[27] Similar trend to DNCB was also observed in the DNAN reduction process, with 2-A-4-NAN as the main intermediate and DAAN as the end product (Fig. 1b and S1b). For DNP reduction, 2-A-4-NP was identified as the main intermediate. However, DAP, the theoretical end product of DNP in ZVI reduction system, was not observed in the effluent of ZVI from HPLC (Fig. 1c and S1c).

In addition, the main reductive products of DNAN, DNCB and DNP were also confirmed by HPLC-MS analysis (Fig. S2). The peaks with retention time of 4.86 min and 2.195 min in Fig. S2(A), were identified as 2-N-4-ACB (m/z=173.1, m/z=175.1) and DACB (m/z=143.1, m/z=145.1), respectively, through MS analysis. Similarly, the peaks with retention time of 3.62 min and 1.87 min in Fig. S2(B), were identified as 2-A-4-NAN (m/z=169.1), and DAAN (m/z=139.1), respectively. After 180 min reaction, the peak with retention time of 8.71 min in Fig. S2(C) was identified as 2-A-4-NP (m/z=163.0), and no DAP was detected in the effluent of ZVI from HPLC-MS analysis.

Accounting for the above intermediate species and end products gave good mass balance (>70% at maximum) for both DNCB and DNAN, but with a reproducible dip at intermediate time (Fig. 1a and 1b), indicating that there was an additional reaction intermediate. This might be due to the formation of nitroso and hydroxylamino compounds as intermediates. Similar result was also reported by Agrawal and Tratnyek.[18] However, these intermediates were hard to detect, as their reduction rate was much faster than their formation rate.[28] Moreover, the conjugation of unstable nitroso and hydroxyamino intermediates often results into the formation of complex azo or azoxy compounds under abiotic conditions.[29] Different from the good mass balance of DNCB and DNAN, poor mass balance (<10% in the end) was observed in the DNP reduction process (Fig. 1c), which was consistent with the continuously decreasing TOC concentration during DNP reduction (Fig. S3). Moreover, the UV-vis spectra evolution during DNP reduction also confirmed the absence of DAP or any other intermediates in the ZVI effluent, as no characteristic absorbance peak could be observed at the end of the reduction process (Fig. S4c). The solution in the DNP reduction system turned from initial light yellow to final reddish black during the reduction process, which illustrated that the reductive products were particularly unstable and could be transformed to unknown products readily.[4,30] Additionally, there was a new unidentified peak in HPLC with retention time of about 4.3 min (Fig. S1c), which possibly corresponded to the polymerization products of the DNP reduction intermediates.

3.2. Kinetics of NACs reduction by ZVI

For the calculation of the rate constants and correlation coefficients (R^2), the NACs reduction data vs *t* were described with pseudo first-order kinetic model (Eq. (2)) and pseudo zero-order kinetic model (Eq. (3)), as was presented in Fig. 2. Obviously, the pseudo first-order kinetics described the reduction of the three NACs by ZVI better, which was indicated by higher correlation coefficients (R^2 of the pseudo first-order kinetics and pseudo zero-order kinetics were 0.9563 and 0.9419, 0.9898 and 0.9065, 0.9650 and 0.8726, for DNCB, DNAN and DNP, respectively). The pseudo first-order rate constants (K_1) were 0.0708 min^{-1} for DNCB, 0.0356 min^{-1} for DNAN and 0.0195 min^{-1} for DNP, following the order of DNCB>DNAN>DNP. Moreover, the better fitting of the three NACs reduction by pseudo first-order kinetics indicated that the removal of three NACs in the ZVI reduction process was significantly affected by the adsorption of the three NACs onto ZVI surface.[23]

The reduction of NACs differed from each other with respect to different molecular configurations of the NACs, such as the charge of the nitrogen atoms, which leaded to different rates of attack by electrons.[31] Since the electron attack was a nucleophilic process, it would occur preferentially at the N atoms with much more positive charge density.[5] As shown in Fig. 3a, the charge densities of the N atoms, which were higher between the two N atoms on DNCB, DNAN and DNP, were 0.218, 0.215 and 0.221, respectively. The order of the reduction rates for DNCB and DNAN was consistent with the order of the charge densities on these N atoms. However, as for DNP, the intramolecular hydrogen bonding, which was formed by the hydroxyl (-OH) substituent group and *ortho*-NO_2 functional group in solution, existed in the molecular structure under the pH condition used in this study.[31] The physicochemical characteristics of NACs was largely dependent on the strength of hydrogen bonding, and the NACs would be more stable due to the presence of intramolecular hydrogen bonding.[31,32] As a result, the electron acceptance by the *ortho*-NO_2 of DNP became more difficult during the reduction by ZVI. Therefore, DNP was reduced at the lowest rate among the three NACs, even though the more positive charge density of the N atoms at the *ortho*-NO_2 position on DNP.

In addition, the mass transfer of NACs to the iron surface might be the reduction rate-limiting step.[19] However, the difference in the functional groups on DNCB, DNAN and DNP (namely chlorine (-Cl), methoxyl ($-OCH_3$) and hydroxyl (-OH), respectively) often resulted into the different physicochemical characteristics of these NACs, such as the octanol/water partition coefficient (K_{ow}), which determines the mass transfer to a large extent.[33] The log K_{ow} of DNCB, DNAN and DNP was 2.17, 1.71 and 1.67, respectively, following in the order of DNCB>DNAN>DNP. The order of the log K_{ow} was also the same as that of the reduction rates, confirming that the adsorption of NACs onto ZVI played a key role during the removal of NACs in the ZVI reduction system.[19]

3.3. Toxicity evaluation during ZVI reduction

The presence of the electron-withdrawing moieties, such as nitro group, often resulted into the high toxicity of the NACs, especially for multi-substituted NACs.[34] Due to the electrophilic nature of the NACs, the mechanistic route for exerting specific toxicity was the attack at electron-rich sites of endogenous macromolecules, resulting in malfunctions of proteins.[35] Therefore, toxicity reduction of the NACs could be achieved by reductive transformation of the electron-withdrawing moieties with ZVI treatment.[4,34]

As shown in Table 1, for the ZVI influent containing 0.5 mM DNCB, DNP or DNAN, the $EC_{50,\ 48h}$ value was 1.3±0.2 %, 2.2±0.3 % and 35.4±0.1 %, respectively. The lower $EC_{50,\ 48h}$ values mean the higher toxicity to Zebrafish. Obviously, the DNCB exhibited the highest acute toxicity, while DNAN exhibited the lowest acute toxicity among the three NACs. After reduction in the ZVI system, the $EC_{50,48h}$ values of the effluent from DNCB and DNAN reduction systems increased to 80.3±3.1 % and 95.7±2.3 %, respectively, suggesting a significant reduction in the biological toxicity. This phenomenon was probably due to the high reductive transformation of NACs during ZVI treatment. Owing to the reduction of the electron-withdrawing nitro groups, the high electron deficiency of the π-electron system on NACs was reduced.[36] In addition, it was found that the TOC concentration decreased slightly in the ZVI systems for DNCB and DNAN (Fig. S3), confirming that the reduction of toxicity was mainly due to the conversion of DNCB and DNAN to their corresponding aromatic amines, not due to the removal of toxic compounds through polymerization, adsorption or deposition on ZVI. However, the effluent of the DNP reduction system was not toxic at all, since all Zebrafish subjected to the undiluted effluents survived. Thus, an $EC_{50,\ 48h}$ values of the effluent from DNP reduction system could not be ascertained. It was mainly due to the formation and precipitation of the reddish black polymeric compounds, which could be observed during the reduction process. For the effluent from DNP reduction system, the low toxicity was consistent with the low concentrations of DNP and its reductive products, as was indicated by the low TOC values (Fig. S3), the poor mass balance (Fig. 1c) and the absence of any characteristic absorbance peak in UV-vis spectra (Fig. S4c).

3.4. Reduction mechanisms of various NACs by ZVI

Based on the intermediate products confirmed by HPLC and HPLC-MS, a possible pathway for the reduction of the three NACs by ZVI was proposed (Fig. 4). In general, the sequential reduction of -NO_2 to -NH_2 included three steps under acid conditions, from nitroso group (-NO) to hydroxylamino group (-NHOH) as intermediates, and eventually to amino group (-NH_2).[20] Nevertheless, due to the presence of different functional groups on DNCB, DNAN and DNP, the reduction of -NO_2 at the *ortho* and the *para* positions for each NAC was not equal during the early stage. DNCB was firstly reduced at *para*-NO_2 position. However, the reduction of DNAN and DNP preferentially occurred at *ortho*-NO_2 position firstly.

^{1}HNMR analysis indicated that chemical shifts of the aromatic proton Ha for DNCB, DNP and DNAN were 7.79, 7.33 and 7.22, respectively (Fig. S5). Larger chemical shift of Ha means stronger electron-withdrawing capacity of functional groups.[37] Thus, the electron-withdrawing ability of functional groups followed in the order of -Cl>-OH>-OCH_3. As a result, the electron-withdrawing functional group (-Cl) on DNCB might strongly deactivate the *ortho*-NO_2 for ZVI reduction, leading to higher charge density of the N atom at the *para* position. However, the existence of the electron-donating functional groups (namely -OCH_3 and -OH) might result into higher charge density of the N atom at *ortho* position on DNAN and DNP. As shown in Fig. 3a, the charge densities of nitrogen atoms at *para*-NO_2 and *ortho*-NO_2 positions were 0.218 and 0.216, 0.213 and 0.221, 0.211 and 0.215, for DNCB, DNP and DNAN, respectively. The charge densities of nitrogen atoms followed the order of *para* > *ortho* for DNCB, *ortho* > *para* for DNAN and DNP, which was consistent with ^{1}HNMR analysis.

As mentioned above, the electron attack will occur preferentially at the N atoms with much more positive charge density. Thus, according to the density function theory computations analysis, the reduction of -NO_2 group on DNCB was selectively favored at the *para* position, as for DNAN and DNP, the reduction of -NO_2 group preferentially occurred at *ortho* position. This theoretical calculation analysis was consistent with the results of the ZVI reduction experiment. It indicated that the selective reduction of the three NACs could be well explained by their difference in the functional groups, which directly affected charge density distribution of the N atoms on the benzene rings. Moreover, as a quantitative description parameter of chemical bonds, bond order has been widely used to understand the nature of molecular electronic structure and predict the molecular reactivity, aromaticity and stability.[38] Lower bond order means higher activity, where bond rupture occurs more easily. Obviously, the N-O mayer bond order (MBO) at *para* and *ortho* positions followed the order of *ortho* > *para* for DNCB, *ortho* < *para* for DNAN and DNP (Fig. 3b), which was also consistent with the results of the reduction experiments.

However, the performance, kinetics and mechanisms of NACs reduction may be affected by the type or characteristics of the ZVI used. Oh et al. has found that the kinetics, mechanism, and pathway of 2,4-dinitrotoluene (DNT) reduction is significantly different between high-purity iron powder and scrap iron.[39] The authors hypothesized that exposed graphite in scrap iron transferred reductants from iron to adsorbed nitroaromatic molecules. Graphite-mediated, indirect reduction of DNT occurred primarily through reduction of the *ortho* nitro group to form 2-amino-4-nitrotoluene (2A4NT), whereas DNT reduction at the iron surface occurred via para nitro reduction to give 4-amino-2-nitrotoluene (4A2NT). However, since the focus of our study was mainly on the effect of molecular structure in the reduction of NACs by ZVI, ZVI powder, which was commonly used for ZVI reduction, was chosen as reductant in this study. Further study is needed for examine the effect of the type or characteristics of the ZVI on NACs reduction.

4. Conclusions

A comprehensive comparison of performance, kinetics, toxicity and mechanisms was conducted for various multi-substituted NACs removal by ZVI in this study. The results indicated that three typical multi-substituted NACs, namely DNCB, DNAN and DNP, could be effectively reduced by ZVI. The reduction process of the three

NACs could be well simulated by pseudo first-order kinetics. The reduction rates of the three NACs followed in the order of DNCB>DNAN>DNP, which was further confirmed by density function theory computations analysis. Moreover, the acute toxicity of the three NACs effluent significantly decreased after treatment by ZVI. Additionally, the mechanism investigation revealed that the selective reduction of nitro groups on the three NACs was closely related to the characteristic of the functional groups on the benzene rings.

Acknowledgments

This research is financed by Innovation Program of Foundation Product, Major Project of Water Pollution Control and Management Technology of P. R. China (No. 2012ZX07101-003-001), National Natural Science Foundation of China (No. 51378261), Zijin Intelligent Program of NJUST (No. 2013-ZJ-02-19), and Research Innovation Grant for Graduate of Jiangsu Common High School (GXZZ13-0225).

Supplementary Information

Evolution of HPLC chromatogram for the three NACs during ZVI reduction process: (a) DNCB; (b) DNAN and (c) DNP (Fig. S1); HPLC-MS spectra of the reductive products of three NACs by ZVI: (A) DNCB; (B) DNAN and (C) DNP (Fig. S2); TOC profiles during the reduction of DNCB, DNAN and DNP in the ZVI system (Fig. S3); Evolution of UV-vis spectra for the three NACs during ZVI reduction process: (a) DNCB; (b) DNAN and (c) DNP (Fig. S4); ^{1}HNMR spectrum of the three standard NACs: (a) DNP; (b) DNCB and (c) DNAN (Fig. S5).

References

1 J.C. Spain, *Annu. Rev. Microbiol.*, 1995, **49**, 523-555.

2 C.X. Yuan, Y.R. Fan, H.X. Guo, J.X. Zhang, Y.L. Wang, D.L. Shan, X.Q. Lu, *Biosens. Bioelectron.*, 2014, ***58***, 85-91.

3 H. Lin, L. Zhu, X. Xu, L. Zang, Y. Kong, J. Chem. Technol. Biot., 2011, **86**,

290-298.

4 J. Shen, C. Ou, Z. Zhou, J. Chen, K. Fang, X. Sun, J. Li, L. Zhou, L. Wang, *J. Hazard. Mater.*, 2013, **260**, 993-1000.

5 J. Shen, Y. Zhang, X. Xu, C. Hua, X. Sun, J. Li, Y. Mu, L. Wang, *Water Res.*, 2013, **47**, 5511-5519.

6 D.T. Sponza, Ö.S. Kuşçu, *Process Biochem.*, 2005, **40**, 1679-1691.

7 M. Barreto-Rodrigues, F.T. Silva, T.C.B. Paiva, *J. Hazard. Mater.*, 2009, **165**, 1224-1228.

8 W.A. Arnold, A.L. Roberts, *Environ. Eng. Sci.*, 2000, **17**, 291-302.

9 H.Y. Shu, M.C. Chang, C.C. Chen, P.E. Chen, *J. Hazard. Mater.*, 2010, **184**, 499-505.

10 J.Z. Bandstra, R. Miehr, R.L. Johnson, P.G. Tratnyek, *Environ. Sci. Technol.*, 2005, **39**, 230-238.

11 A. Koutsospyros, J. Pavlov, J. Fawcett, D. Strickland, B. Smolinski, W. Braida, *J. Hazard. Mater*. 2012, **219**, 75-81.

12 A. Sinha, P. Bose, *J. Colloid Interface Sci.*, 2007, **314**, 552-561.

13 A. Sinha, P. Bose, *Environ. Sci. Pollut. R.*, 2014, **21**, 10442-10452.

14 A. Sinha, P. Bose, *J. Hazard. Mater.*, 2009, **164**, 301-309.

15 N.C. Mueller, J. Braun, J. Bruns, M. Černík, P. Rissing, D. Rickerby, B. Nowack, *Environ. Sci. Pollut. R.*, 2012, **19**, 550-558.

16 C. Le, J. Liang, J. Wu, P. Li, X. Wang, N. Zhu, P. Wu, B. Yang, *Water. Sci. Technol.*, 2011, **64**, 2126-2131.

17 B.T. Oh, C.L. Just, P.J.J. Alvarez, *Environ. Sci. Technol.*, 2001, **35**, 4341-4346.

18 L. Ma, W.X. Zhang, *Environ. Sci. Technol*. 2008, **42**, 5384-5389.

19 A. Agrawal, P.G. Tratnyek, *Environ. Sci. Technol*. 1995, **30**, 153-160.

20 Y. Mu, H.Q. Yu, J.C. Zheng, S.J. Zhang, G.P. Sheng, *Chemosphere*, 2004, **54**, 789-794.

21 Y.Z. Lei, G.H. Zhao, Y.G. Zhang, M.C. Liu, L. Liu, B.Y. Lv, J.X. Gao, *Environ. Sci. Technol*. 2010, **44**, 7921-7927.

22 OECD, Test No. 203: Fish, Acute Toxicity Test, *OECD Publishing*, 1992.

23 M. Hou, F. Li, X. Liu, X. Wang, H. Wan, *J. Hazard. Mater.*, 2007, **145**, 305-314.

24 J. Fan, Y. Guo, J. Wang, M. Fan, *J. Hazard. Mater.*, 2009, **166**, 904-910.

25 G. N. Jovanovic, J. E. Atwater, P. Znidarsic-Plazl, I. Plazl, *Chem. Eng. J.*, 2015, **274**, 50-60.

26 X. Xu, J. Wo, J. Zhang, Y. Wu, Y. Liu, *Desalination*, 2009, **242**, 346-354.

27 J. Shen, Z. Zhou, C. Ou, X. Sun, J. Li, W. Han, L. Zhou, L. Wang, *J. Environ. Sci.*, 2012, **24**, 1900-1907.

28 M.D. Roldán, E. Pérez-Reinado, F. Castillo, C. Moreno-Vivián, *Fems. Microbiol. Rev.*, 2008, **32**, 474-500.

29 C. Y. Wang, D. D. Zheng, J. B. Hughes, Biotechnol. Lett., 2000, **22**, 15-19.

30 L.R. Krumholz, J.M. Suflita, *Anaerobe*, 1997, **3**, 399-403.

31 Y. Liu, H. Liu, J. Ma, X. Wang, *Appl. Catal. B: Environ.*, 2009, **91**, 284-299.

32 Y. Valadbeigi, V. Ilbeigi and M. Tabrizchi, *Comput. Theor. Chem.*, 2015, **1061**, 27-35.

33 J. Radjenouic, A. Bagastyo, R.A. Rozendal, Y. Mu, J. Keller, K. Rabaey, Water Res., 2011, **45**, 1579-1586.

34 X. Xu, H. Lin, L. Zhu, Y. Yang, J. Feng, *J . Chem. Technol. Biot.*, 2011, **86**, 993-1000.

35 H. Schmitt, R. Altenburger, B. Jastorff, G. Schüürmann, *Chem. Res. Toxicol.*, 2000, **13**, 441-450.

36 B.A. Donlon, E. Razo-Flores, J.A. Field, G. Lettinga, *Appl. Environ. Microbiol.*, 1995, **61**, 3889-3893.

37 Y.P. Wang, C.T. Lin, H.Y. Cheng, T.S. Lin, *Inorg. Chim. Acta*, 2013, **394**, 337-347.

38 T. Lu, F. Chen, *J. Phys. Chem. A.*, 2013, **117**, 3100-3108.

39 S. Y. Oh, D. K. Cha and P. C. Chiu, *Environ. Sci. Technol.,* 2002, **36**, 2178-2184.

Figure captions

Figure 1 Concentration evolution of NACs and their corresponding reduction intermediates as a function of reduction time, (a) DNCB; (b) DNAN; (c) DNP.

Figure 2 Reduction kinetics of three NACs: (a) Pseudo first-order kinetic model; (b) Pseudo zero-order kinetic model.

Figure 3 Quantum chemical calculation of DNCB, DNAN and DNP: (a) charge density of the atoms; (b) N-O mayer bond order.

Figure 4 Possible reduction pathways of DNCB, DNAN and DNP by ZVI.

Table 1 The toxicity of the influent and effluent from NACs reduction system

NACs	$EC_{50,48h}$(v/v) of the influent	$EC_{50,48h}$(v/v) of the effluent
DNCB	1.3±0.2 %	80.3±3.1 %
DNAN	35.4±0.1 %	95.7±2.3 %
DNP	2.2±0.3 %	Not toxic*

* All Zebrafish subjected to the undiluted effluent survived.

Fig. 1

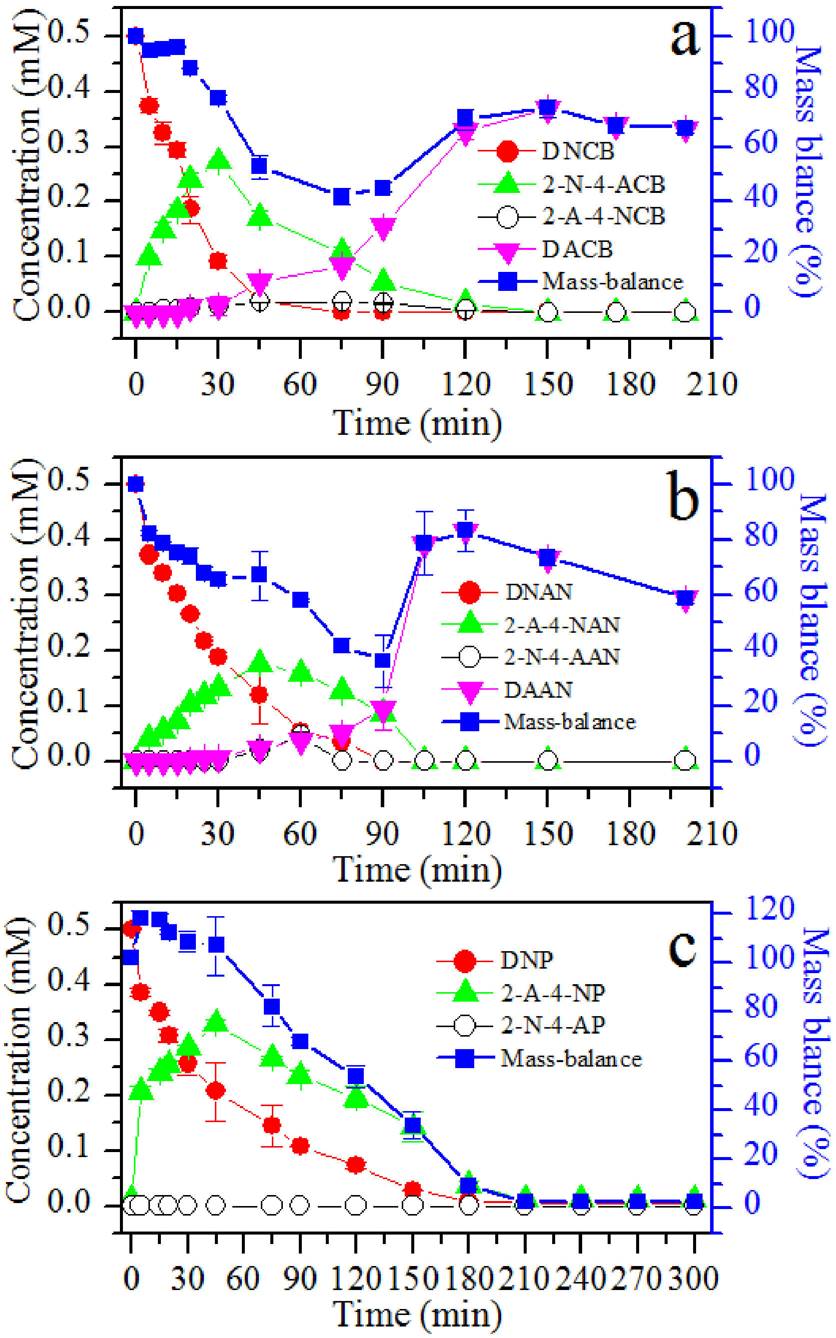
a
Concentration (mM)
0.0
0.1
0.2
0.3
0.4
0.5
Mass blance (%)
0
20
40
60
80
100
Time (min)
0
30
60
90
120
150
180
210
DNCB
2-N-4-ACB
2-A-4-NCB
DACB
Mass-balance
b
DNAN
2-A-4-NAN
2-N-4-AAN
DAAN
Mass-balance
c
120
240
270
300
DNP
2-A-4-NP
2-N-4-AP
Mass-balance

Fig. 2

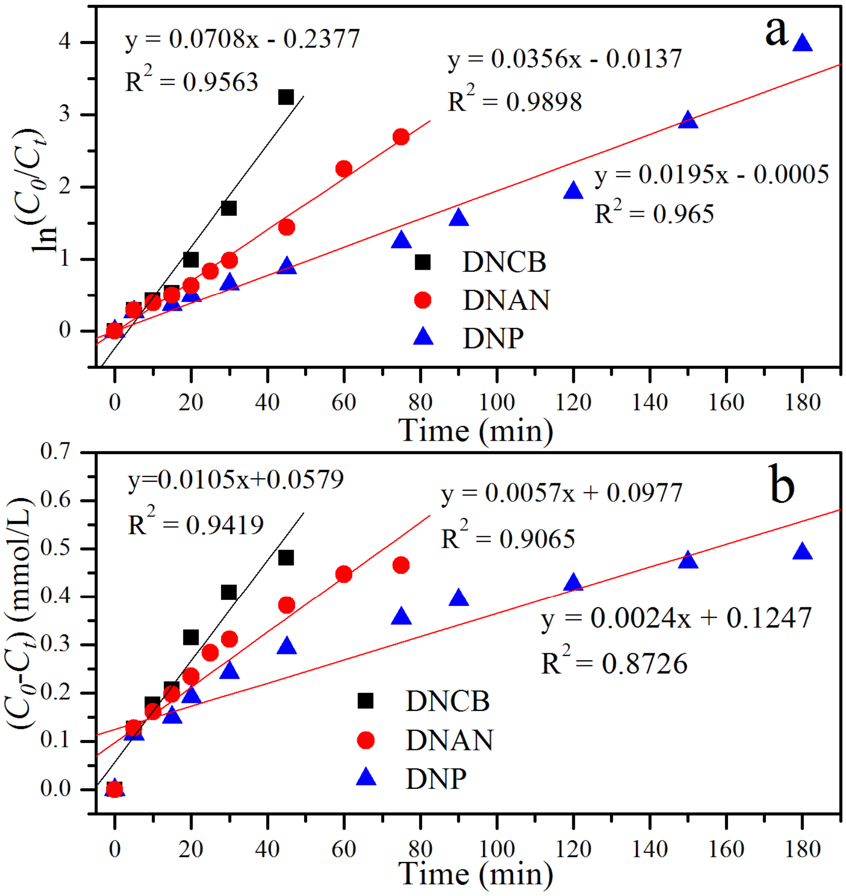
a
y = 0.0708x - 0.2377
R^2 = 0.9563
y = 0.0356x - 0.0137
R^2 = 0.9898
y = 0.0195x - 0.0005
R^2 = 0.965
■ DNCB
● DNAN
▲ DNP
$\ln(C_0/C_t)$
0
1
2
3
4
0
20
40
60
80
100
120
140
160
180
Time (min)
b
y=0.0105x+0.0579
R^2 = 0.9419
y = 0.0057x + 0.0977
R^2 = 0.9065
y = 0.0024x + 0.1247
R^2 = 0.8726
■ DNCB
● DNAN
▲ DNP
$(C_0\text{-}C_t)$ (mmol/L)
0.0
0.1
0.2
0.3
0.4
0.5
0.6
0.7
0
20
40
60
80
100
120
140
160
180
Time (min)

Fig. 3

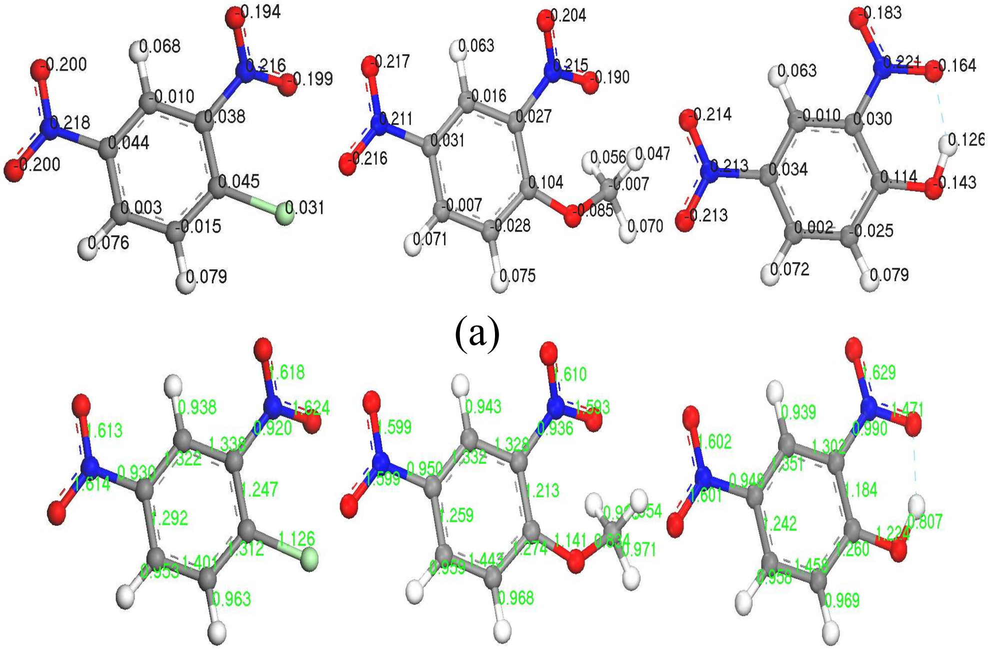
-0.194
0.068
-0.200
0.216
-0.199
-0.010
0.038
0.218
0.044
-0.200
0.045
0.031
0.003
-0.015
0.076
0.079
-0.204
0.063
-0.217
0.215
-0.190
-0.016
0.027
0.211
0.031
-0.216
0.056
0.047
0.104
-0.007
-0.085
0.070
-0.007
0.071
-0.028
0.075
-0.183
0.063
0.221
-0.164
-0.214
-0.010
0.030
0.126
0.213
0.034
0.114
-0.143
-0.213
0.002
-0.025
0.072
0.079
1.618
0.938
1.624
1.613
1.336
0.920
0.930
1.322
1.614
1.247
1.292
1.126
1.312
0.953
1.401
0.963
1.610
0.943
1.593
1.599
1.328
0.936
0.950
1.332
1.599
1.213
1.259
1.141
1.274
0.971
0.959
1.443
0.968
1.629
0.939
1.471
1.602
1.302
0.990
0.948
1.351
1.601
1.184
1.242
0.807
1.224
1.260
0.958
1.458
0.969

(a)

(b)

Fig. 4

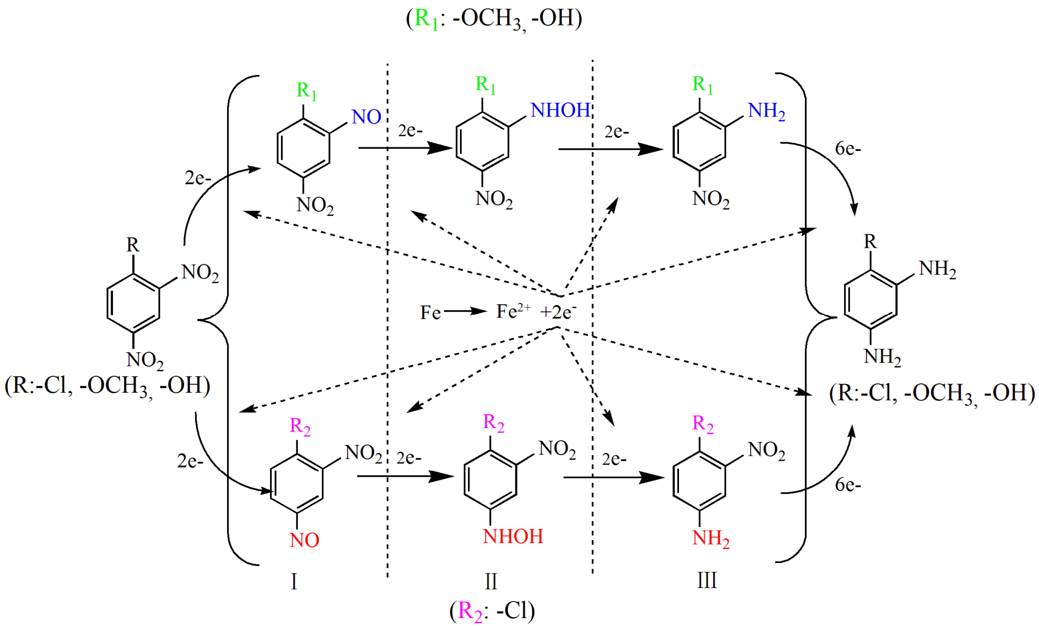
(R_1: -OCH_3, -OH)
R_1
NO
NO_2
2e-
R_1
NHOH
NO_2
2e-
R_1
NH_2
NO_2
6e-
2e-
R
NO_2
NO_2
(R:-Cl, -OCH_3, -OH)
Fe → Fe^{2+} +$2e^-$
R
NH_2
NH_2
(R:-Cl, -OCH_3, -OH)
2e-
R_2
NO_2
NO
2e-
R_2
NO_2
NHOH
2e-
R_2
NO_2
NH_2
6e-
I
II
III
(R_2: -Cl)